EUROPEAN ORGANIZATION FOR NUCLEAR RESEARCH

# A SEARCH FOR NARROW RESONANCES IN PROTON-PROTON COLLISIONS AT 53 GeV CENTRE OF MASS ENERGY

M.G. Albrow, B. Alper, J. Armitage, D. Aston, P. Benz, G.J. Bobbink, B. Bošnjaković[1)], A.G. Clarke, F.C. Erné, W.M. Evans, C.N.P. Gee, E.S. Groves[2)], L.E. Holloway[3)], J.N. Jackson, G. Jarlskog, H. Jensen, P. Kooijman, D. Korder, F.K. Loebinger, A.A. Macbeth, N.A. McCubbin, H.E. Montgomery, J.V. Morris, P.G. Murphy, H. Ogren[4)], R.J. Ott, D. Radojicic[5)], S. Rock, A. Rudge, J.C. Sens, A.L. Sessoms[6)], J. Singh, D. Stork, P. Strolin[7)], J. Timmer, W.A. Wenzel[2)]

CERN, Geneva, Switzerland
Daresbury Laboratory, U.K.
Foundation for Fundamental Research on Matter (F.O.M.), The Netherlands
University of Lancaster, U.K.
University of Liverpool, U.K.
University of Manchester, U.K.
Rutherford Laboratory, U.K.
University of Utrecht, The Netherlands
University of Lund, Sweden

## Abstract

A search for narrow resonances produced in pp collisions at the CERN ISR has been carried out using two magnetic spectrometers to measure and identify two final state charged hadrons. The resultant two particle invariant mass spectra show no strong structure suggesting any new narrow resonance. The statistical significance of various enhancements seen in the data is discussed, and upper limits on the cross-section times branching ratio for new particle production are presented.

Submitted to Nuclear Physics, Geneva, June 1976

Present addresses:

1) Sector Straling, Ministerie van Volksgezondheid en Milieuhygiëne, Leidschendam, The Netherlands.
2) Lawrence Berkeley Lab., Berkeley, CA 94720, U.S.A.
3) University of Illinois, Champaign, Urbana, IL 61801, U.S.A.
4) Indiana University, Bloomington, IN 47401, U.S.A.
5) Department of Nuclear Physics, Keble Road, Oxford, OX1 3RH, England.
6) Harvard University, Cambridge, MA 02138, U.S.A.
7) E.T.H., Hönggerberg, 8049 Zürich, Switzerland.

## Introduction

An experiment has been performed at the CERN Intersecting Storage Rings to search for new states, produced in pp collisions, which decay into two charged hadrons - $\pi^{\pm}$, $K^{\pm}$, p and $\bar{p}$. Such new states would be of considerable interest in view of the theoretical speculations stimulated by the discovery of the J/$\psi$ particle[1].

## Apparatus and Data Acquisition

The apparatus consisted of two single-arm magnetic spectrometers shown schematically in fig. 1. The small angle spectrometer (SAS) accepted particles of one sign of charge produced at 50 ± 5 mrad above one of the circulating beams. The momenta of the accepted particles lay between 3 and 15 GeV, and three threshold gas Cerenkov counters were used to identify pions, kaons, and protons over this momentum range. The SAS solid angle is $\sim$ 0.08 msr, and the momentum resolution is $\delta p/p \sim 1.2\%$ (FWHM). The SAS is described in more detail in ref. 2. The wide angle spectrometer (WAS) accepted simultaneously both positively and negatively charged particles produced at $38 \pm 5^0$ (85% of the data) or $45 \pm 5^0$ (15% of the data) to the acute bisector of the two beams. Two threshold gas Cerenkov counters and a time of flight system were used to identify pions, kaons, and protons over the momentum range 0.5 to 3.4 GeV, except for a K/p ambiguity in the region 1.4 to 1.65 GeV. The WAS solid angle is $\sim$ 11 msr, and the momentum resolution is $\delta p/p \sim 0.03$ p (GeV) FWHM. The WAS is described in more detail in ref. 3. Complementary to the two spectrometers is a scintillation counter hodoscope system which covers about 97% of the solid angle around the intersection region. This hodoscope system is described in ref. 4.

Both these spectrometers have been fully operational for some time, and their properties are well understood. The present experiment required only the implementation of a hardware trigger to operate the two spectrometers in coincidence, and the installation of a pair of spark chambers in front of the first WAS Cerenkov counter to improve the resolution of the production angle of the WAS particle, and hence

of the invariant mass of the two hadron system. This mass resolution is calculated to be between 10 and 20 MeV (standard deviation) depending on the mass. The overall systematic error on the mass scale is estimated to be not more than 25 MeV.

In a period of 460 hours of data taking, corresponding to an integrated luminosity of 8.0 $10^{36}cm^{-2}$, a total of $\sim$ 840 K coincidence triggers were recorded of which 177 K had a reconstructed and uniquely identified track in each spectrometer. 17% of the integrated luminosity was with positively charged particles accepted in SAS, and the rest with negatively charged particles. All data were taken at s = 2760 $GeV^2$, i.e. 26.5 GeV momentum in each ring. In terms of the 4-momentum of the two hadron state, obtained by summing the 4-momenta of the SAS and WAS particles, the data lie in the range $0.15 \lesssim x \lesssim 0.6$ where $x = 2p_L/\sqrt{s}$, $0.3 \lesssim p_T \lesssim 2.0$ GeV, and the invariant mass range is $\sim$ 2 GeV extending up from some lower limit (1 to 2 GeV) which depends on the SAS and WAS particle masses.

## Results

The data comprise 21 distinct two hadron combinations, $h_1h_2$, after combining $h_1(SAS)h_2(WAS)$ with $h_1(WAS)h_2(SAS)$. Plotting out these 21 invariant mass spectra in 20 MeV bins, we nowhere observe a narrow enhancement so large as to render arguments about statistical significance superfluous.

In order to analyse the statistical significance of the various fluctuations seen in the $\sim$ 1600 20 MeV mass bins making up the 21 plots, it is essential to know, with high precision, the shape of the mass spectrum resulting from the independent, non-resonant, emission of two hadrons from the collision. To estimate the shape of this continuum for any $h_1(SAS)h_2(WAS)$ combination we generate a mass spectrum by making all possible non-coincident $h_1(SAS)h_2(WAS)$ combinations. Using data taken in the coincidence mode, rather than with SAS and WAS operating independently, we automatically take account of the average effect of the weak kinematic correlation resulting from the coincidence requirement. All spectrometer acceptance effects are also incorporated in the mass

spectra obtained.

The spectrum generated for each $h_1 h_2$ combination is then normalized to the number of $h_1 h_2$ coincident events. As the non-coincident spectrum is known with very high statistical precision we can estimate $\chi$, the number of standard deviations of the coincident events from the non-resonant continuum, by:

$$\chi = \frac{n_C - n_{NC}}{\sqrt{n_{NC}}}$$

where $n_C$ is the number of coincident events in the bin, and $n_{NC}$ is the normalized number of non-coincident events. Where necessary adjacent bins are combined until $n_C \geq 5$.

The 21 mass distributions are shown in fig. 2a) - u). Indicated are the coincident events (histogram), the normalized non-coincident spectrum (drawn lines), and the value of $\chi$ in each bin is plotted below. The 'double hump' structure seen in some of the plots, e.g. fig. 2l), is a consequence of the different mass acceptance for $h_1(\text{SAS})h_2(\text{WAS})$ and $h_1(\text{WAS})h_2(\text{SAS})$. As remarked above, the data show no strong structure, e.g. with a strength like the J/$\psi$ signal seen in the BNL experiment. Indeed a striking feature of the data is the close overall agreement between the coincident and non-coincident event spectra. In the region of phase space covered by this experiment there appears to be little, if any, difference between the mass distributions of two hadrons which originate from the same or different pp collisions. It is furthermore clear that the very high multiplicity of typical pp collisions at this energy ($p_{LAB} \sim$ 1500 GeV) constitutes a major combinatorial background in searching for non-leptonic decays of possible narrow resonances.

In more detail, the spectra of coincident events show deviations from the non-coincident spectra. The statistical significance of the deviations is illustrated in fig. 3 which shows the $\chi^2$ distribution obtained from the 21 plots of fig. 2 and, superimposed, the theoretical distribution for 1 degree of freedom normalized to the total number

of bins in fig. 2. For $\chi^2 \lesssim 10$, at which point the theoretical curve falls below 0.1 per bin, the two distributions can be seen to agree, indicating that the great majority of the deviations observed are in accord with what one would expect on statistical grounds.

Details of the four effects seen with $\chi^2 = \chi_0^2 > 10$ are given in the inset of fig. 3. They occur in $p\pi^-$ at 1750 MeV (fig.2p) , pp at 3330 MeV (fig. 2t) , $pK^-$ at 2150 MeV (fig. 2q) , and $\pi^+\pi^+$ at 3530 MeV (fig. 2g , insert). The $p\pi^-$ effect is a dip below the expected level and thus of no interest. For each of these effects we compute the confidence level, CL, from the Poisson distribution*:

$$CL = \sum_{n=0}^{n_1} \frac{(n_{NC})^n e^{-n_{NC}}}{n!} + \sum_{n=n_2}^{\infty} \frac{(n_{NC})^n e^{-n_{NC}}}{n!}$$

Here $n_{NC}$ is, as above, the expected number of events from the non-coincident spectrum, and $n_1$ and $n_2$ are, respectively, the smaller and larger solutions of $\chi_0^2 = (n-n_{NC})^2/n_{NC}$. Multiplying CL by the total number of bins gives the number of bins expected to have $\chi^2 \geq \chi_0^2$. For the three effects which show a positive enhancement above the expected level, the expected number of bins is 2.2, 2.2 and 1.0 to be compared with the observed number of bins 3,2 and 1. One concludes that the effects observed in pp at 3330 MeV, $pK^-$ at 2150 MeV, and $\pi^+\pi^+$ at 3530 MeV are compatible with statistical fluctuations even though the $\chi^2$'s are large.

Nevertheless, it should perhaps be remarked that a signal in the $pK^-$ channel at 2150 MeV could be readily accommodated in charm theories[5]. There is a well established $\Lambda$ resonance at a mass of 2100 MeV which is

* Even for $n_{NC}$ as large as 50, the Gaussian and Poisson distributions differ significantly at large $\chi^2$. For $\chi^2 \lesssim 5$ and $n_{NC} > 10$ the two distributions agree closely. Hence the theoretical $\chi^2$ distribution drawn in fig. 3 is the one derived from a Gaussian distribution, whilst we use the Poisson distribution for bins with $\chi^2 > 10$.

however broad - $\Gamma \sim 120$ MeV. The probability that such a broad resonance would show up in one 20 MeV bin is negligibly small.

We have also looked for broad enhancements in the data. The most significant is a four-bin effect in $K^-K^-$ centred at 2340 MeV ($n_C = 17$, $n_{NC} = 5.6$). However the $K^-K^-$ data is sparse (see fig. 2f) and it is hard to know if the non-coincident spectrum is correct in this case. The next most significant three effects are : $\pi^+K^+$ centred at 1780 MeV (fig. 2c, $n_C = 195$, $n_{NC} = 150$), $p\pi^-$ centred at 2660 MeV (fig. 2p, $n_C = 768$, $n_{NC} = 675$) and $\pi^+\pi^-$ centred at 2570 MeV (fig. 2i, $n_C = 190$, $n_{NC} = 147$). The enhancement in $p\pi^-$ could correspond to the $N^*(2650)$ resonance, though it appears to be narrower than the reported width of $\sim 300$ MeV. The absence of $N^*$'s in the data, with the possible exception of the $N^*(2650)$, could be explained by the peripheral nature of their production, with momenta which lie beyond the acceptance of the apparatus.

Next we examine the possibility that some new narrow resonance might exist in several charge states, almost degenerate in mass, which decay into several different two hadron combinations $h_1h_2$. We have therefore combined the data into five sets, distinguished only by baryon number, B = - 2, - 1, 0, + 1, + 2. The B = - 2 and + 2 combinations are the pp and $\bar{p}\bar{p}$ combinations shown in fig. 2t) and u) respectively. The other three (B = -1, +1, 0) are shown in fig. 4a) to c), and the $\chi^2$ distribution for the entire data grouped in this way (i.e. from fig. 2t) and u) and fig. 4a) to c)) is shown in fig. 5. Once again the overall agreement between the coincident and non-coincident spectra is very good, as is that between the observed $\chi^2$ distribution and the theoretically expected one. We are left with two effects with $\chi^2 > 10$ which are detailed in the inset of fig. 5. The first is a repetition of the pp effect detailed in fig. 3. The second ($\chi^2 = 15.1$) is seen in the B = + 1 channel at a mass of 3510 MeV. It thus arises from combining the four $h_1h_2$ combinations $p\pi^+$, $p\pi^-$, $pK^-$, $pK^+$. No significant enhancement is seen at this mass in the B = - 1

spectrum, but the statistics are much poorer. The mass region around 3500 MeV of the B = + 1 spectrum is shown on an enlarged scale in the inset of fig. 4b, and table I lists the contributions of the four contributing channels. The dominant contributions are from the $p\pi$ channels. Interpreted as a statistical fluctuation, this enhancement is a 1 in 10 chance (see inset of fig. 5).

We are left with the possibility of making cuts in various kinematic variables of the two hadron system, and/or on the associated charge multiplicity measured in the complementary hodoscope system. The nature of the acceptance of the two spectrometers is such that the Feynman x and transverse momentum, $p_T$, of the two hadron system are essentially linearly related to the mass, and so cuts on x or $p_T$ are tantamount to mass cuts. The solid angle coverage in the rest frame of the two hadron system is too restricted to look for possible indications of resonance production in the decay angular distribution.

We have tried to reduce the combinatorial background by cutting on the total associated multiplicity and by cutting on the associated multiplicity in the hemisphere containing the SAS and WAS particles. We have also tried to enhance possible diffractive production by requiring only one particle at a small production angle in the hemisphere opposite the SAS and WAS particles. All these multiplicity cuts only produce pro rata reductions in the statistics.

In order to obtain upper limits on the cross-section times branching ratio, $\sigma.BR$, for new particle production, the acceptance of the SAS-WAS apparatus has been calculated allowing for particle decay and absorption. Uncertainties in this calculation and in the overall normalization could lead to a systematic uncertainty of a factor $\sim 2$ in the cross-sections. We obtain the invariant cross-section times branching ratio, $E \frac{d^3\sigma}{dp^3} . BR$, by assuming isotropic decay in the rest frame of the two hadrons, and $\sigma.BR$ using a parametrization of the differential cross-section proposed by Bourquin and Gaillard[6], namely:

$$E\frac{d^3\sigma}{dp^3} \propto \frac{f(y)}{\{(p_T^2 + M^2)^{\frac{1}{2}} + 2(\text{GeV})\}^{12.3}} \begin{cases} \exp(-p_T) & ; \; p_T < 1 \text{ GeV} \\ \exp(-23(p_T - 1)s^{-\frac{1}{2}} - 1) & ; \; p_T > 1 \text{ GeV} \end{cases}$$

where $f(y) = \exp(-5.13/Y^{0.38})$ ; $Y = y_{max}(p_T) - y$

M is the mass of the two hadron system, and $p_T$ and y are respectively its transverse momentum and rapidity in the pp centre of mass. This parametrization gives a good description of central production over a wide range of energies. For combinations with baryon number $\geq 1$ we make rough allowance for leading particle effects by setting $f(y) = 1$.

With these assumptions, the various enhancements discussed above yield the values of $E\frac{d^3\sigma}{dp^3}$.BR and $\sigma$.BR listed in table IIa. To define upper limits for new particle production we take 5 standard deviations above the normalized continuum level, and some typical values are listed in table IIb. The upper limits on $E\frac{d^3\sigma}{dp^3}$.BR tend to lie in the range 1 to 10 $\mu$b GeV$^{-2}$ at $x \sim 0.3$ and $p_T \sim 1$ GeV. Kinoshita et al.[7] have calculated the differential cross-section for inclusive charmed meson production to be $E\frac{d^3\sigma}{dp^3} \sim 0.5$ $\mu$b GeV$^{-2}$ at these values of x, $p_T$ and s.

The 5 standard deviation upper limits on $\sigma$.BR are shown as a function of mass, for all combinations, in fig. 6a) to f) - the various combinations being grouped together as in fig. 2. Over the region of reasonable acceptance these upper limits are $\sim 0.1$ mb. Sivers[8] has suggested cross-sections of $\sim$100 $\mu$b for charm production in pp collisions at $\sqrt{s}$ = 53 GeV. Aubert et al.[9] have measured two hadron mass spectra and obtained limits in the range $\sigma$.BR $\sim 10^{-7}$ mb in proton proton collisions at $\sqrt{s}$ = 7.5 GeV. Bleser at al.[10] have obtained $\sigma$.BR $\sim 10^{-4}$ mb in neutron proton collisions at $\sqrt{s}$ = 20 GeV.

The upper limits obtained in this experiment for the production of new narrow resonances leave room for charm production at a level suggested by theory.

Acknowledgements

It is a pleasure to acknowledge the excellent running conditions provided at the ISR during the taking of this data. The mass histograms presented in this paper were drawn using the CERN graphics package GD3.

This experiment was supported by the Swedish Atomic Research Council, the Stichting voor Fundamenteel Onderzoek der Materie (F.O.M.), which is supported by the Nederlandse Organizatie voor Zuiver Wetenschappelijk Onderzoek (Z.W.O.), and the U.K. Science Research Council through the Daresbury and Rutherford Laboratories.

References

1) J.J. Aubert, U. Becker, P.J. Biggs, J. Burger, M. Chen, G. Everhart, P. Goldhagen, J. Leong, T. McCorriston, T.G. Rhoades, M. Rohde, Samuel C.C. Ting, Sau Lan Wu, and Y.Y. Lee, Phys. Rev. Lett. 33, 1404 (1974).

J.E. Augustin, A.M. Boyarski, M. Breidenbach, F. Bulos, J.T. Dakin, G.J. Feldman, G.E. Fischer, D. Fryberger, G. Hanson, B. Jean-Marie, R.R. Larsen, V. Lüth, H.L. Lynch, D. Lyon, C.C. Morehouse, J.M. Paterson, M.L. Perl, B. Richter, P. Rapidis, R.F. Schwitters, W.M. Tanenbaum, F. Vannucci, G.S. Abrams, D. Briggs, W. Chinowsky, C.E. Friedberg, G. Goldhaber, R.J. Hollebeek, J.A. Kadyk, B. Lulu, F. Pierre, G.H. Trilling, J.S. Whitaker, J. Wiss, and J.E. Zipse, Phys. Rev. Lett. 33, 1406 (1974).

For a recent theoretical review, see:
H.Harari Proceedings of the 1975 International Symposium on Lepton and Photon Interactions at High Energies. p.317 SLAC 1975.

2) M.G. Albrow, D.P. Barber, A. Bogaerts, B. Bošnjaković, J.R. Brooks, A.B. Clegg, F.C. Erné, C.N.P. Gee, A.D. Kanaris, A. Lacourt, D.H. Locke, F.K. Loebinger, P.G. Murphy, A. Rudge, J.C. Sens, K. Terwilliger, and F. van der Veen, Phys. Lett. 42B, 279 (1972).

3) B. Alper, H. Bøggild, P. Booth, L.J. Carroll, G. von Dardel, G. Damgaard, B. Duff, J.N. Jackson, G. Jarlskog, L. Jönsson, A. Klovning, L. Leistam, E. Lillethun, S. Olgaard-Nielsen, M. Prentice, and J.M. Weiss, Nucl. Phys. B87, 19 (1975).

4) M.G. Albrow, D.P. Barber, P. Benz, B. Bošnjaković, J.R. Brooks, C.Y. Chang, A.B. Clegg, F.C. Erné, P. Kooijman, F.K. Loebinger, N.A. McCubbin, P.G. Murphy, D. Radojicic, A. Rudge, J.C. Sens, A.L. Sessoms, J. Singh, P. Strolin, and J. Timmer, Nucl. Phys. B102, 275 (1976).

5) See for example:
M.K.Gaillard, B.W.Lee, and J.L.Rosner, Rev. Mod. Phys. 47, 277 (1975)

6) M. Bourquin and J.M. Gaillard, submitted to Nuclear Physics.

7) K. Kinoshita, M. Mizouchi, T. Tashiro, and H. Noda, University of Bielefeld, preprint Bi-75/12.

8) D. Sivers, Nucl. Phys. B106, 95 (1976).

9) J.J. Aubert, U. Becker, P.J. Biggs, J. Burger, M. Chen, G. Everhart, J. Leong, T.G. Rhoades, M. Rohde, T. Sanford, Samuel C.C. Ting, W.H. Toki, Sau Lan Wu, J.W. Glenn III and Y.Y. Lee, Phys. Rev. Lett. 35, 416 (1975).

10) E.J. Bleser, B. Gobbi, L. Kenah, J. Keren, J. Rosen, R. Ruchti, H. Scott, D. Spelbring, J. Biel, C. Bromberg, T. Ferbel, P. Slattery, D. Underwood and D. Freytag, Phys. Rev. Lett. 35, 76 (1975).

TABLE I

Contributions to enhancement in B=+1 spectrum at 3510 ± 10 MeV.

| Channel | $n_C$ | $n_{NC}$ | $\chi$ |
|---|---|---|---|
| $p\pi^+$ | 17 | 9.9 | + 2.26 |
| $p\pi^-$ | 27 | 16.7 | + 2.51 |
| $pK^+$ | 4 | 3.3 | + 0.38 |
| $pK^-$ | 6 | 2.1 | + 2.69 |
| $\Sigma$ | 54 | 32 | + 3.89 |

$n_C$ is the number of coincident events seen, and $n_{NC}$ is the number expected from the normalized non-coincident spectra.

TABLE II

a) Cross-section values for the various enhancements discussed in the text.

| Channel | Mass(MeV) | x | $p_T$(GeV) | $E\frac{d^3\sigma}{dp^3}$ .BR μb $GeV^{-2}$ | σ.BR mb |
|---|---|---|---|---|---|
| pp | 3330 | 0.4 | 0.75 | 4.5 | 0.22 |
| $pK^-$ | 2150 | 0.3 | 0.55 | 20 | 0.57 |
| $\bar{p}K^+$ | 2150 | 0.3 | 0.55 | 1.2 | 0.035 |
| $\pi^+\pi^+$ | 3530 | 0.54 | 2.1 | 0.77 | 1.3 |
| $p\pi^-$ | 2620-2700 | 0.4 | 0.85 | 8.6 | 0.45 |
| B=+1 | 3510 | 0.45 | 1.0 | 0.23 | 0.016 |

TABLE II (continued)

b) 5 standard deviation upper limits on cross-sections for new particle production.

| Channel | Mass(MeV) | x | $p_T$(GeV) | $E\frac{d^3\sigma}{dp^3}$.BR μb GeV$^{-2}$ | σ.BR mb |
|---|---|---|---|---|---|
| $K^+\pi^-$ | 2000 | 0.3 | 0.73 | 5.7 | 0.41 |
| | 2500 | 0.38 | 1.1 | 1.5 | 0.29 |
| | 3000 | 0.43 | 1.4 | 0.60 | 0.21 |
| $K^-\pi^+$ | 2000 | 0.32 | 0.73 | 2.1 | 0.17 |
| | 2500 | 0.41 | 1.15 | 0.55 | 0.14 |
| | 3000 | 0.45 | 1.4 | 0.30 | 0.11 |
| $pK^-$ | 2000 | 0.26 | 0.50 | 52 | 1.35 |
| | 2500 | 0.26 | 0.55 | 4.9 | 0.15 |
| | 3000 | 0.32 | 0.71 | 1.4 | 0.06 |
| $\bar{p}K^+$ | 2000 | 0.21 | 0.5 | 5.85 | 0.18 |
| | 2500 | 0.30 | 0.85 | 0.51 | 0.044 |
| | 3000 | 0.36 | 1.25 | 0.38 | 0.076 |
| $\pi^+\pi^-$ | 2000 | 0.35 | 0.91 | 4.2 | 0.57 |
| | 2500 | 0.40 | 1.20 | 1.4 | 0.36 |
| | 3000 | 0.45 | 1.52 | 0.45 | 0.22 |
| | 3500 | 0.53 | 2.1 | 0.2 | 0.31 |
| $K^+K^-$ | 2000 | 0.29 | 0.59 | 7.2 | 0.38 |
| | 2500 | 0.37 | 0.97 | 1.0 | 0.15 |
| | 3000 | 0.44 | 1.3 | 0.50 | 0.16 |
| $p\bar{p}$ | 3000 | 0.30 | 0.70 | 1.3 | 0.083 |
| | 3500 | 0.37 | 0.96 | 0.34 | 0.046 |
| | 4000 | 0.49 | 1.15 | 0.66 | 0.21 |

Figure captions

Fig. 1 Sketch of the apparatus showing the Small Angle Spectrometer (SAS) positioned above the downstream arm of one of the beams, and the Wide Angle Spectrometer (WAS) positioned in the plane defined by the two proton beams. S2, BM1, BM2, BM3, and $BM_W$ indicate magnets; C1, C2, C3, $C1_W$, and $C2_W$ indicate gas Cerenkov counters.

Fig. 2 Two hadron invariant mass spectra for the 21 $h_1h_2$ combinations. The data are plotted in 20 MeV bins. Through each histogram is drawn the normalized curve obtained from non-coincident events, and below is plotted the value of $\chi$ in each bin. The $\chi^2$ per degree of freedom is also given for each plot.

| | | | |
|---|---|---|---|
| a) to d) | $\lvert S \rvert = 1$ mesons | | $K^+\pi^-$, $\pi^-K^-$, $\pi^+K^+$, $\pi^+K^-$ |
| e) to h) | $\lvert Q \rvert = 2$ mesons | | $\pi^-\pi^-$, $K^-K^-$, $\pi^+\pi^+$, $K^+K^+$ |
| i) to k) | Q=0,S=0 | | $\pi^+\pi^-$, $K^+K^-$, $p\bar{p}$ |
| l) to o) | B = - 1 | | $\bar{p}\pi^-$, $\bar{p}K^-$, $\bar{p}\pi^+$, $\bar{p}K^+$ |
| p) to s) | B = + 1 | | $p\pi^-$, $pK^-$, $p\pi^+$, $pK^+$ |
| t), u) | $\lvert B \rvert = 2$ | | $pp$, $\bar{p}\bar{p}$ |

Fig. 3 $\chi^2$ frequency distribution for the 21 plots of fig. 2, and, superimposed, the theoretical $\chi^2$ distribution for 1 degree of freedom normalized to 1617. Details of the 4 effects with $\chi^2 > 10$ are given in the inset.

Fig. 4 Two hadron invariant mass spectra for the data combined according to Baryon number B.

a) B = - 1

b) B = + 1

c) B = 0

Fig. 5 $\chi^2$ frequency distribution for the data combined into 5 sets, B=-2, -1, 0, +1, +2. Superimposed is the theoretical $\chi^2$

distribution for 1 degree of freedom normalized to 505. Details of the 2 effects seen with $\chi^2 > 10$ are given in the inset.

Fig. 6 5 s.d. upper limits on $\sigma$.BR as a function of mass for the 21 $h_1 h_2$ combinations.

a) $|S| = 1$ mesons

b) $|Q| = 2$ mesons

c) $Q=0$, $S=0$ mesons

d) $B = -1$

e) $B = +1$

f) $|B| = 2$

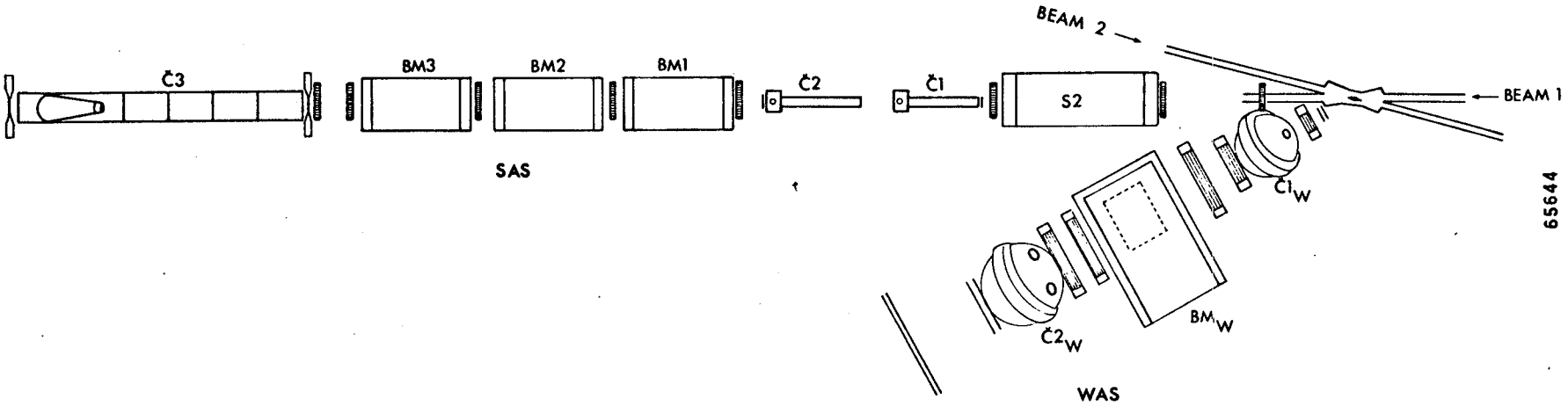


Fig.1

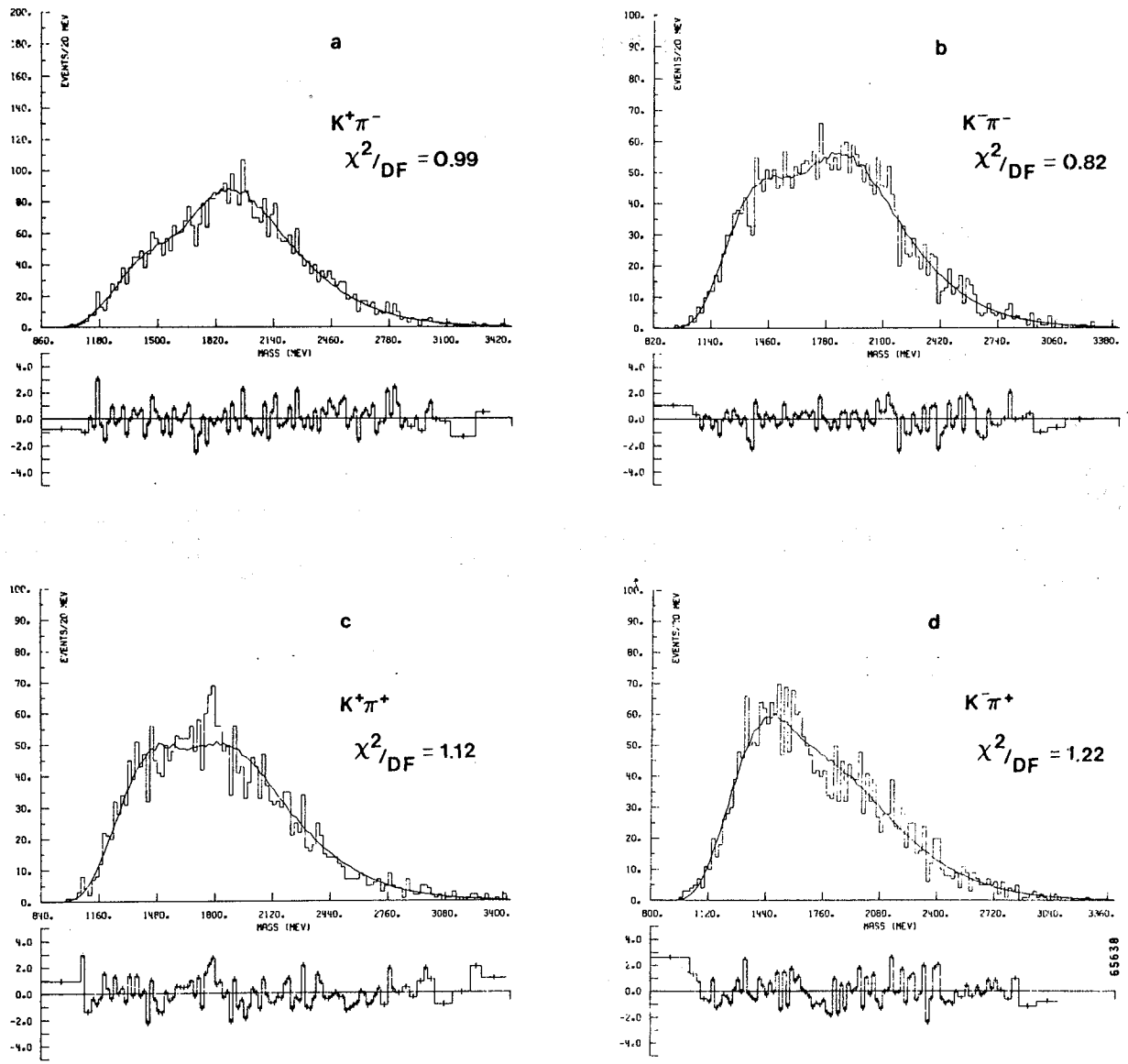
a
$K^+\pi^-$
$\chi^2/_{DF} = 0.99$
b
$K^-\pi^-$
$\chi^2/_{DF} = 0.82$
c
$K^+\pi^+$
$\chi^2/_{DF} = 1.12$
d
$K^-\pi^+$
$\chi^2/_{DF} = 1.22$
EVENTS/20 MEV
MASS (MEV)
65638

Fig.2 a)

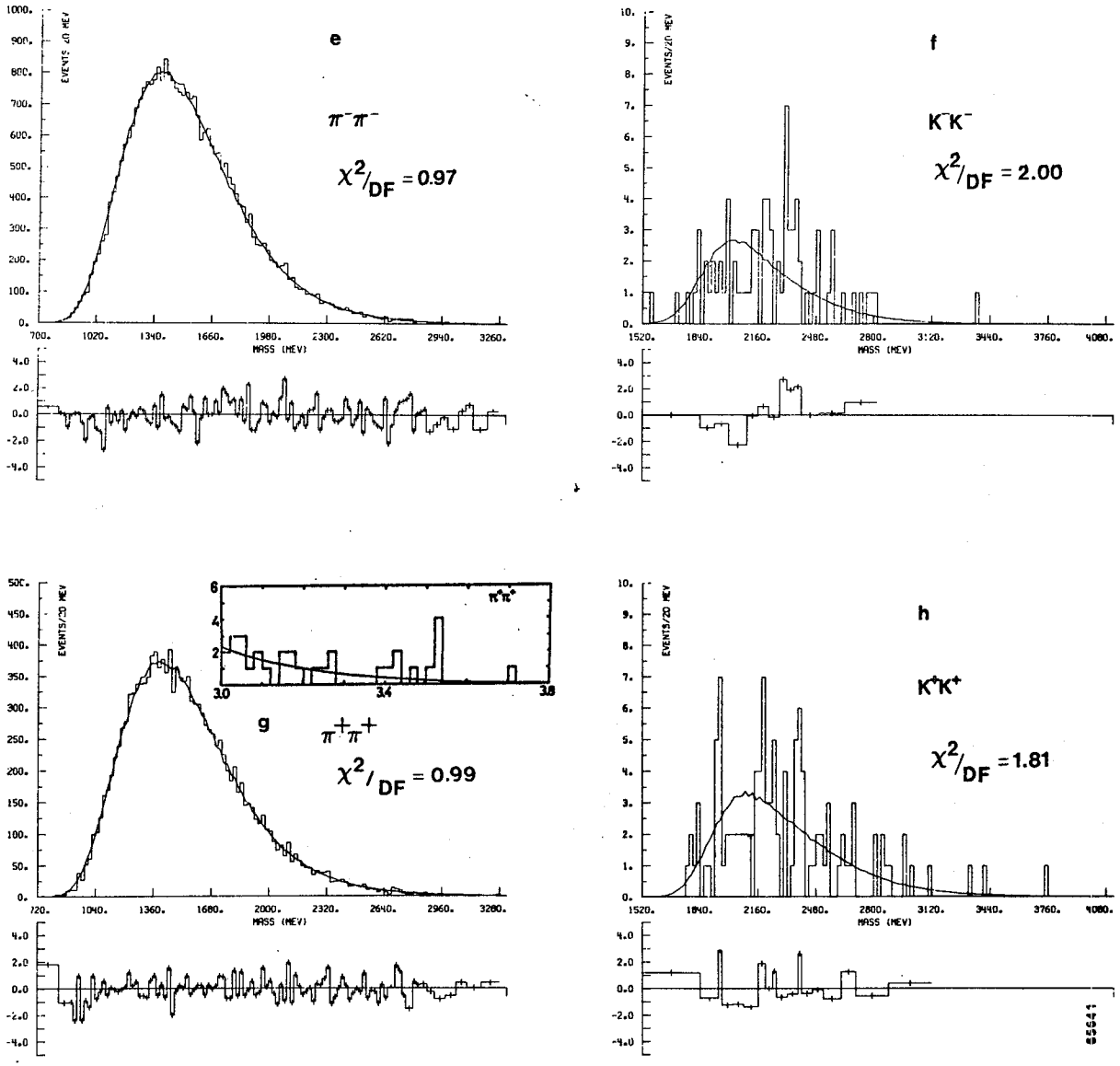
e
$\pi^-\pi^-$
$\chi^2/_{DF} = 0.97$
f
$K^-K^-$
$\chi^2/_{DF} = 2.00$
g
$\pi^+\pi^+$
$\chi^2/_{DF} = 0.99$
h
$K^+K^+$
$\chi^2/_{DF} = 1.81$
EVENTS/20 MEV
MASS (MEV)

Fig.2 b)

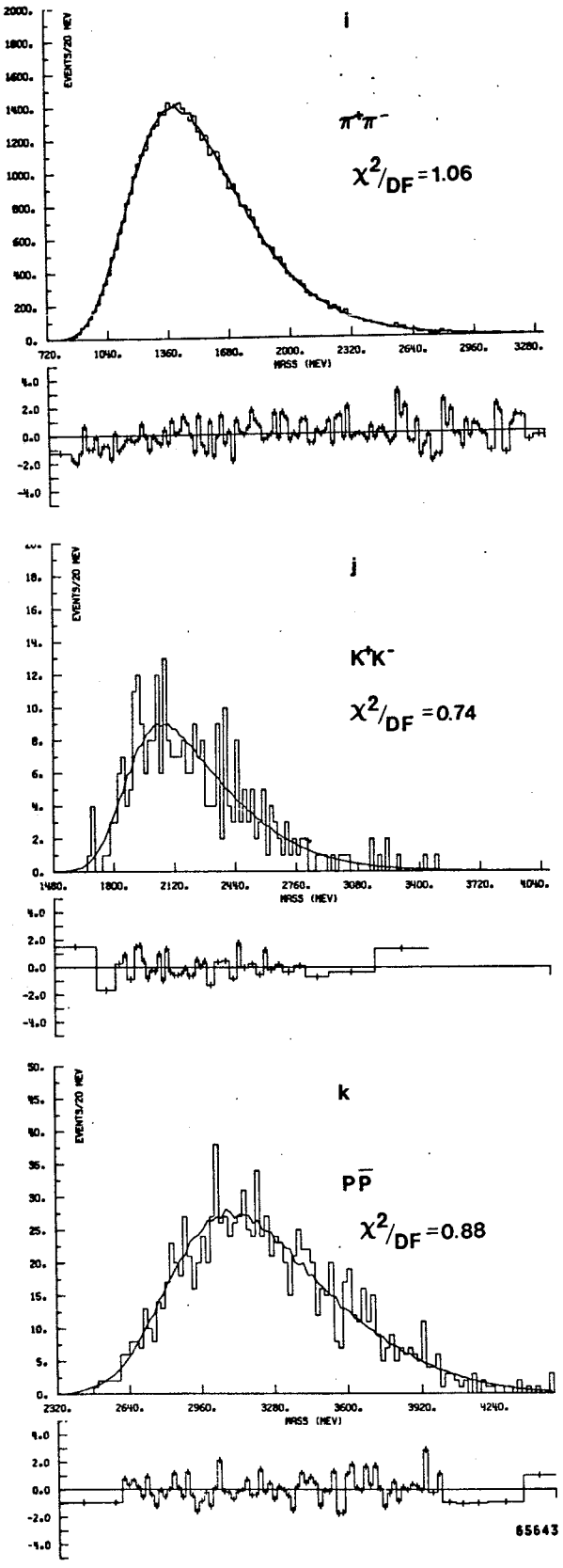
i
$\pi^+\pi^-$
$\chi^2/DF = 1.06$
EVENTS/20 MEV
MASS (MEV)
j
$K^+K^-$
$\chi^2/DF = 0.74$
EVENTS/20 MEV
MASS (MEV)
k
$P\bar{P}$
$\chi^2/DF = 0.88$
EVENTS/20 MEV
MASS (MEV)
85643

Fig.2 c)

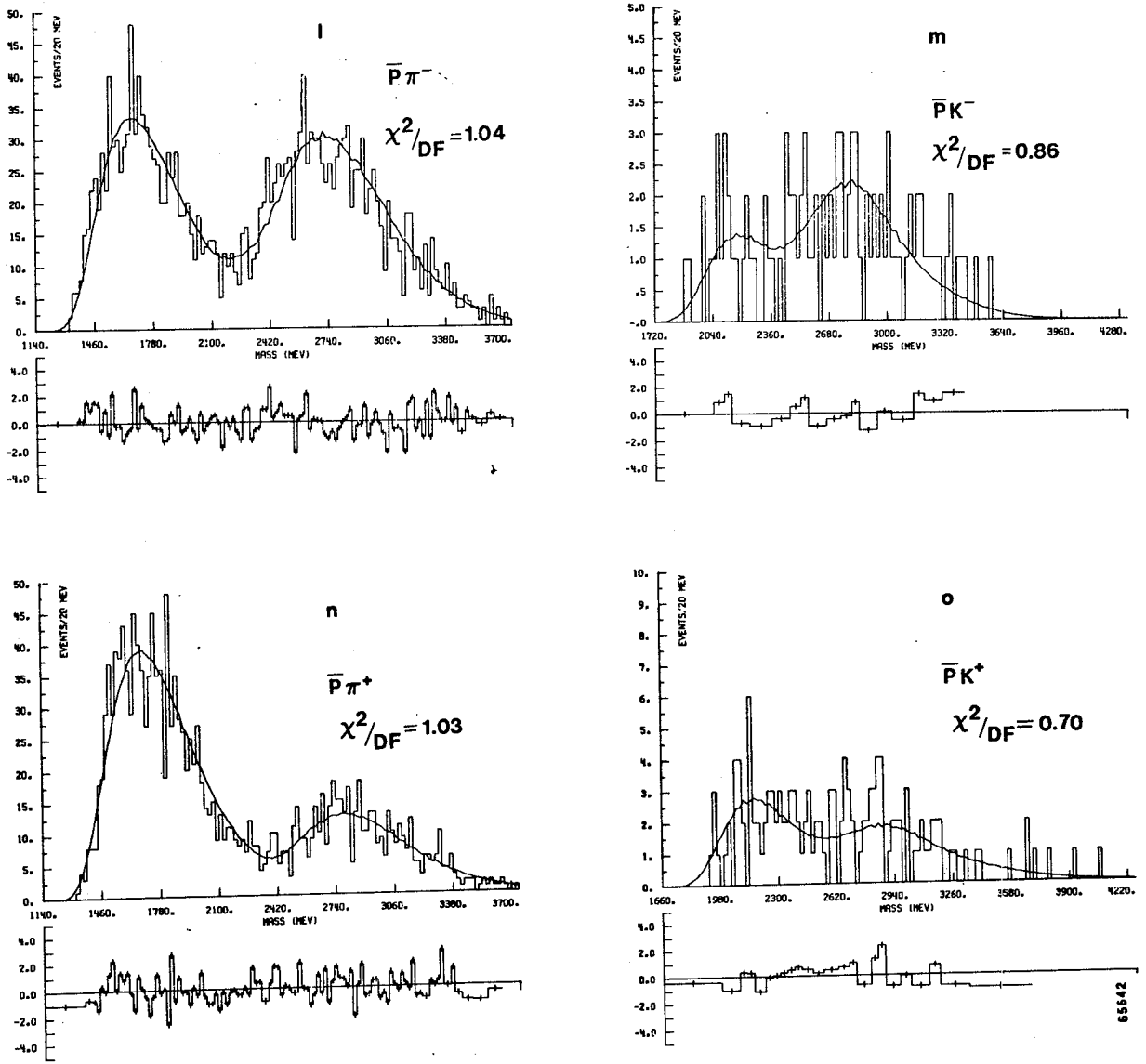
l
$\bar{P}\pi^-$
$\chi^2/_{DF}$=1.04
m
$\bar{P}K^-$
$\chi^2/_{DF}$=0.86
n
$\bar{P}\pi^+$
$\chi^2/_{DF}$=1.03
o
$\bar{P}K^+$
$\chi^2/_{DF}$=0.70
EVENTS/20 MEV
MASS (MEV)
65642

Fig.2 dj

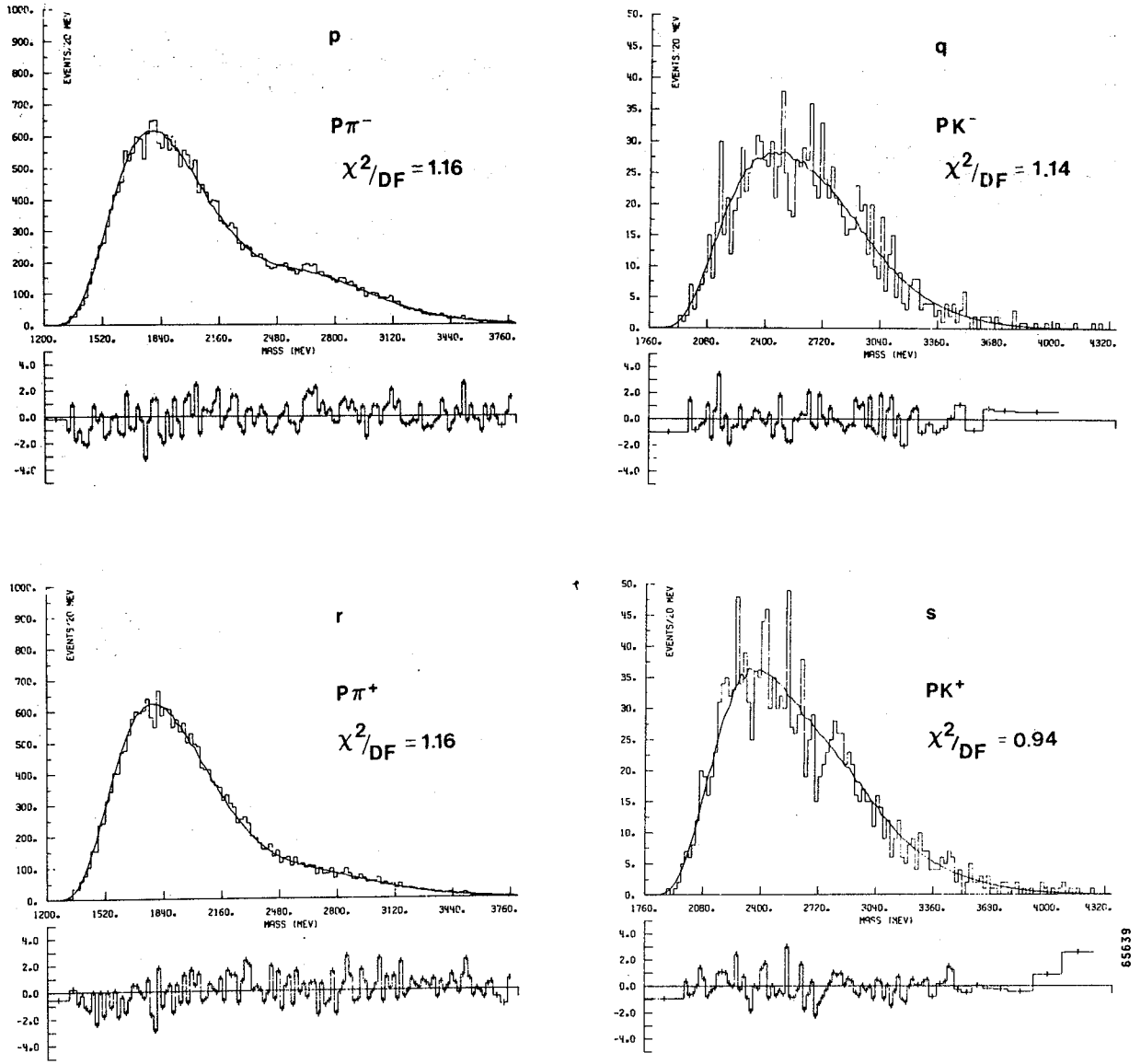
p
$P\pi^-$
$\chi^2/DF = 1.16$
q
$PK^-$
$\chi^2/DF = 1.14$
r
$P\pi^+$
$\chi^2/DF = 1.16$
s
$PK^+$
$\chi^2/DF = 0.94$
MASS (MEV)
65639

Fig.2

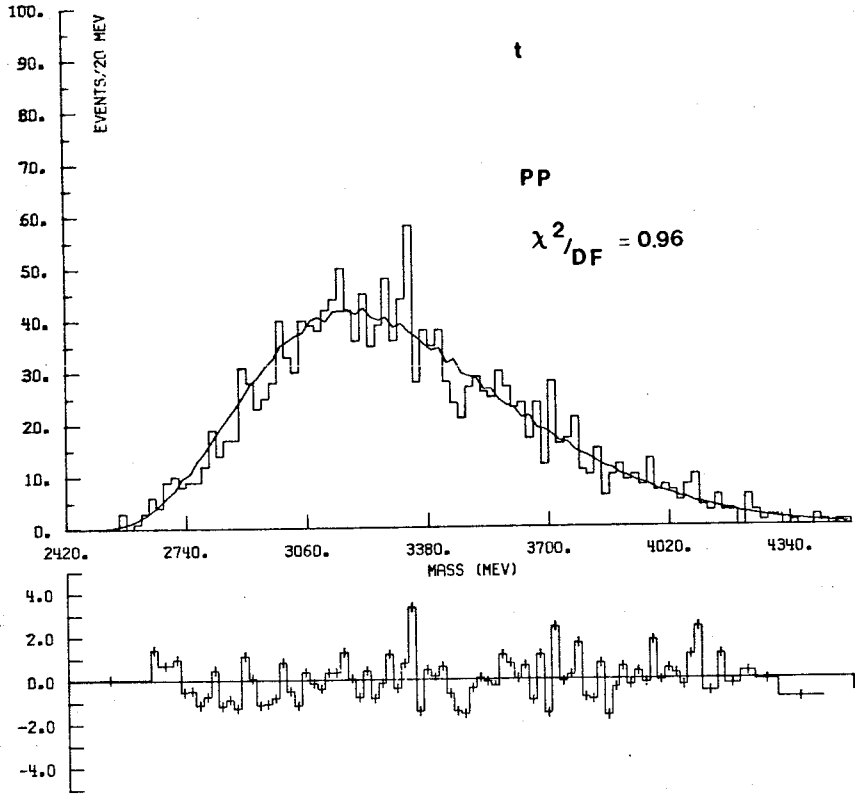
t
PP
$\chi^2/_{DF}$ = 0.96
EVENTS/20 MEV
MASS (MEV)

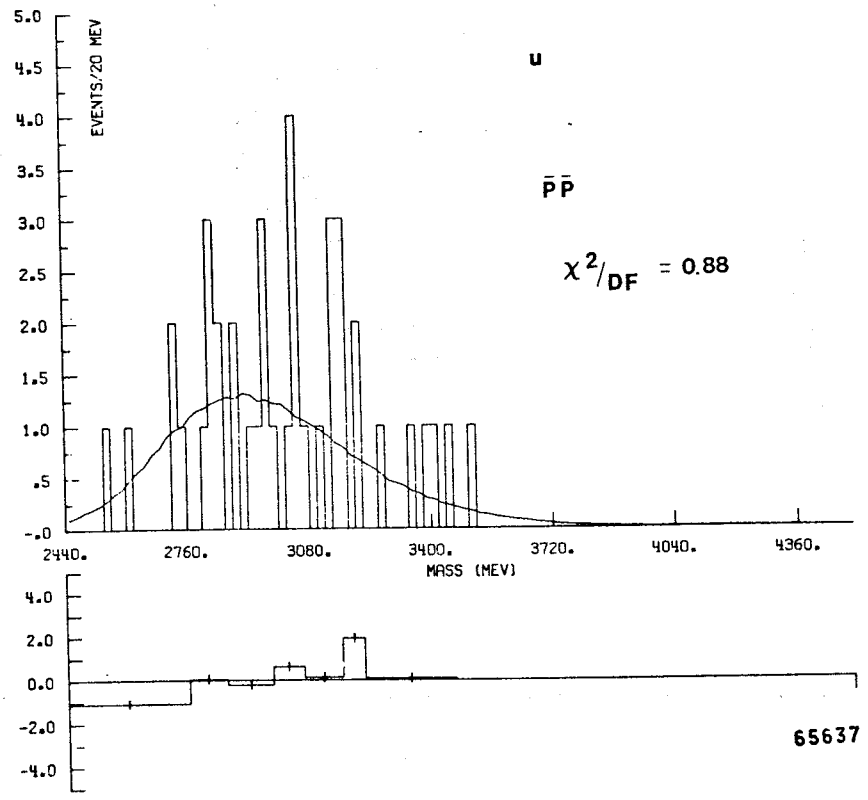
u
$\bar{P}\bar{P}$
$\chi^2/_{DF}$ = 0.88
EVENTS/20 MEV
MASS (MEV)
65637

Fig.2

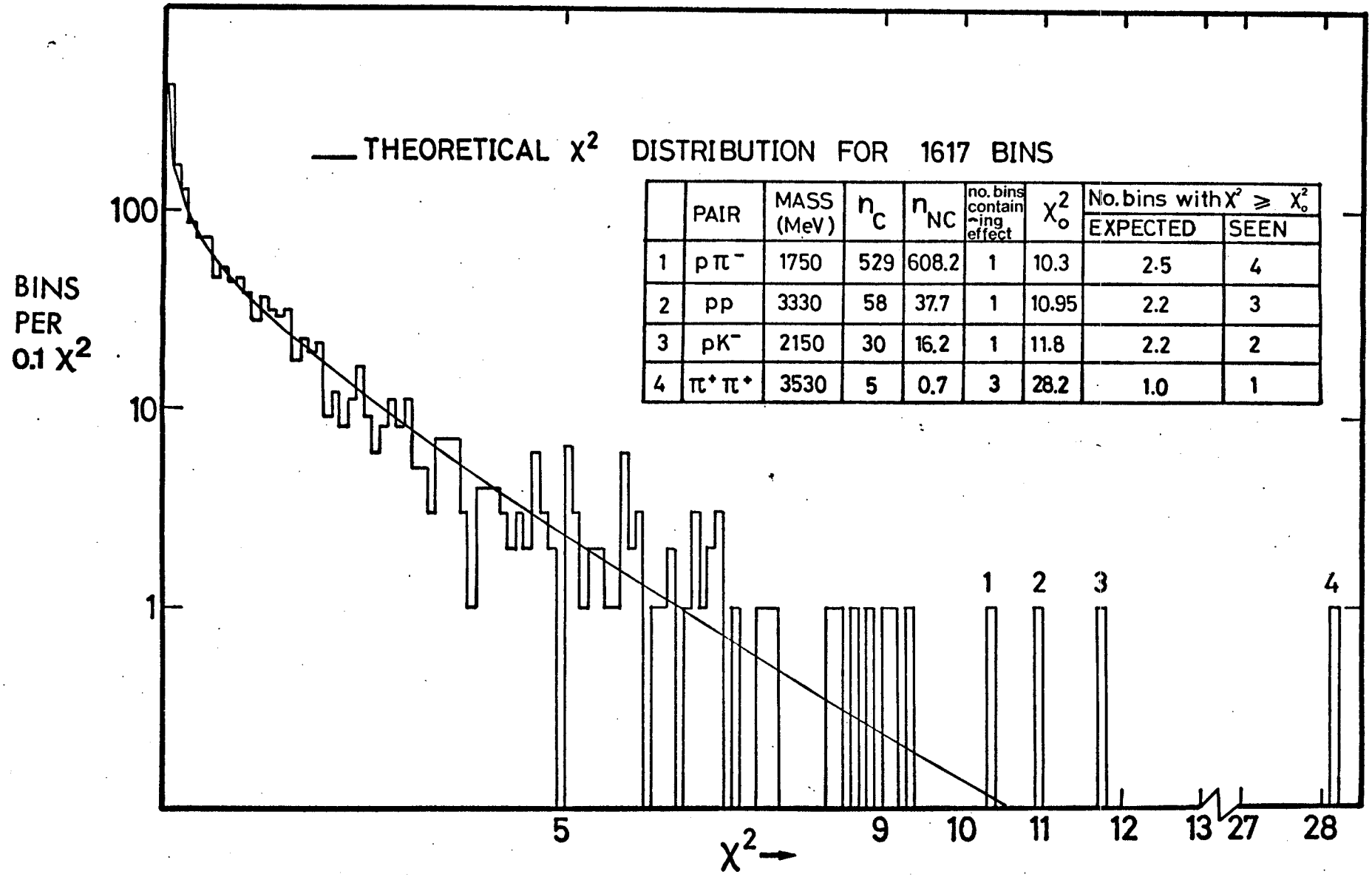


| | PAIR | MASS (MeV) | $n_C$ | $n_{NC}$ | no. bins containing effect | $\chi^2_o$ | No. bins with $\chi^2 \geq \chi^2_o$ | |
|---|---|---|---|---|---|---|---|---|
| | | | | | | | EXPECTED | SEEN |
| 1 | $p\pi^-$ | 1750 | 529 | 608.2 | 1 | 10.3 | 2·5 | 4 |
| 2 | $pp$ | 3330 | 58 | 37.7 | 1 | 10.95 | 2.2 | 3 |
| 3 | $pK^-$ | 2150 | 30 | 16.2 | 1 | 11.8 | 2.2 | 2 |
| 4 | $\pi^+\pi^+$ | 3530 | 5 | 0.7 | 3 | 28.2 | 1.0 | 1 |

Fig. 3

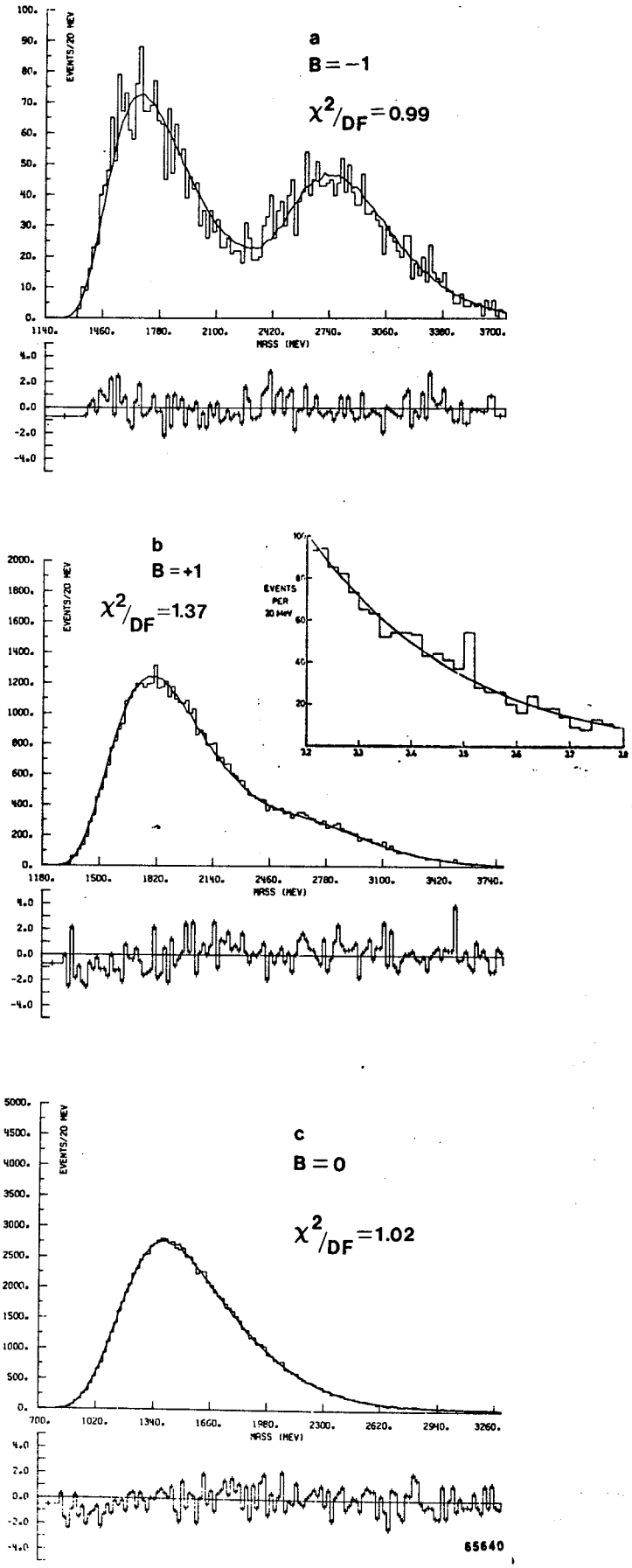
a
B = −1
$\chi^2/DF = 0.99$
EVENTS/20 MEV
MASS (MEV)
b
B = +1
$\chi^2/DF = 1.37$
EVENTS PER 20 MeV
c
B = 0
$\chi^2/DF = 1.02$
65640

Fig.4

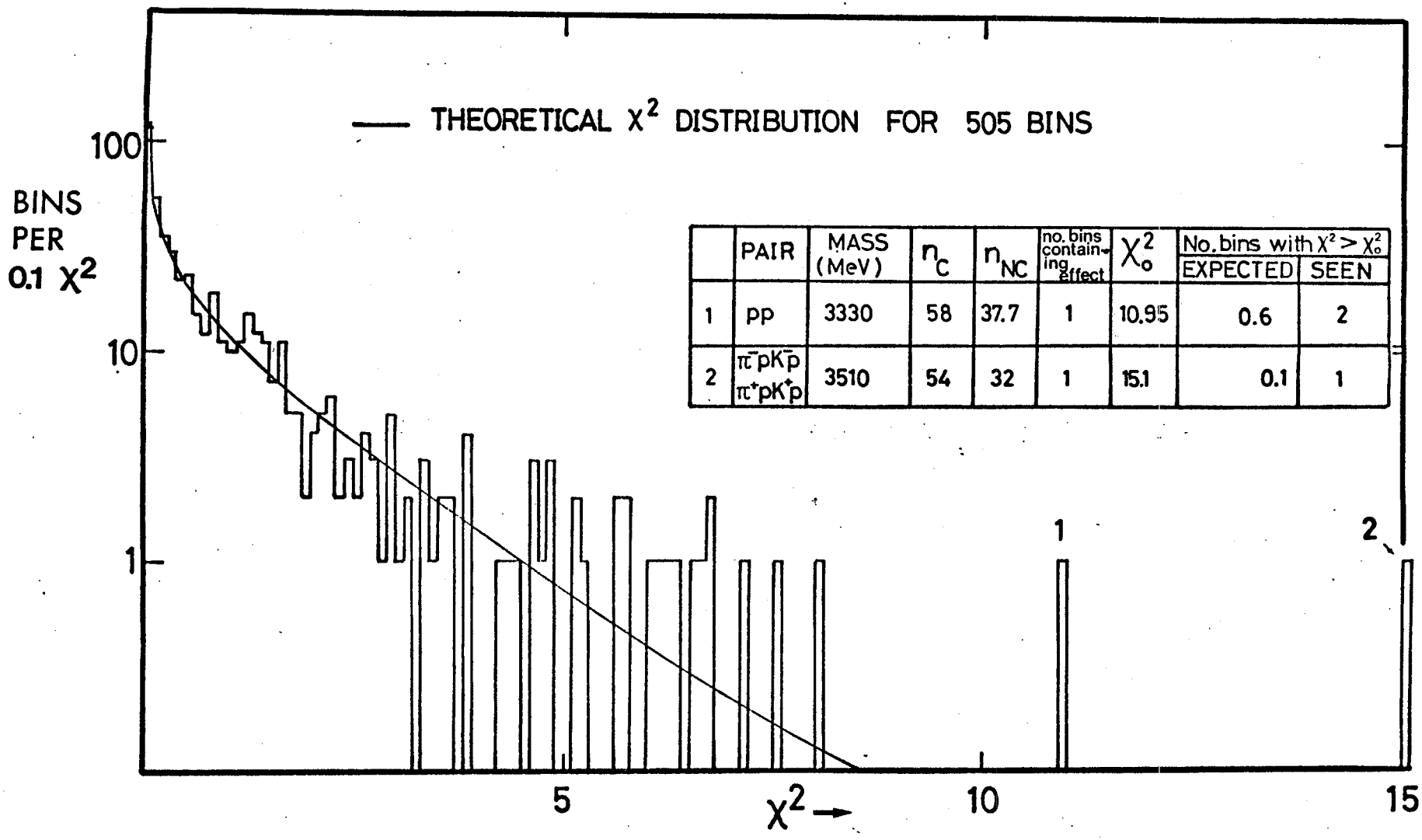


| | PAIR | MASS (MeV) | $n_C$ | $n_{NC}$ | no. bins containing effect | $\chi^2_o$ | No. bins with $\chi^2 > \chi^2_o$ | |
|---|---|---|---|---|---|---|---|---|
| | | | | | | | EXPECTED | SEEN |
| 1 | pp | 3330 | 58 | 37.7 | 1 | 10.95 | 0.6 | 2 |
| 2 | $\pi^-pK^-p$ $\pi^+pK^+p$ | 3510 | 54 | 32 | 1 | 15.1 | 0.1 | 1 |

Fig. 5

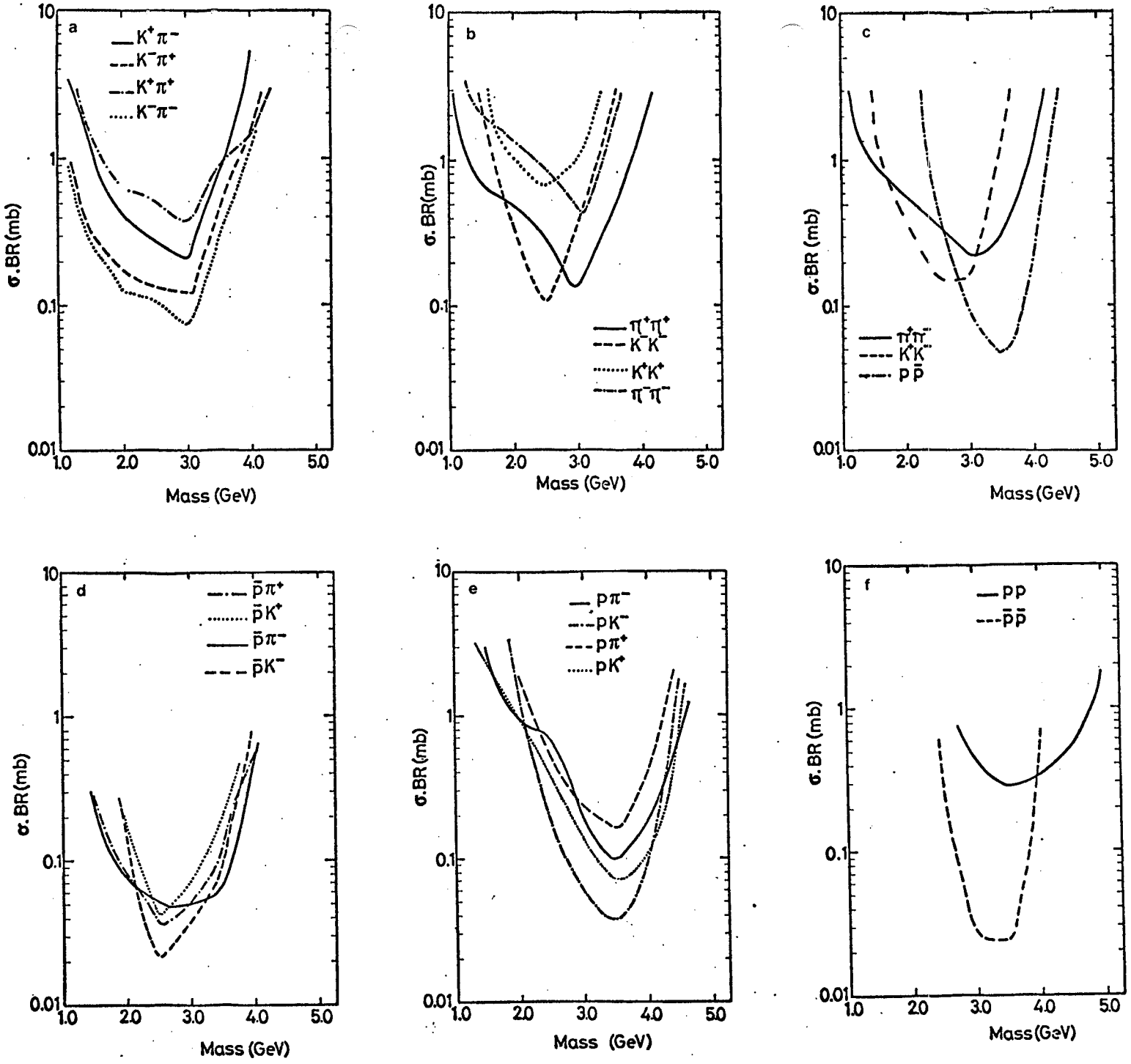
a
$K^+\pi^-$
$K^-\pi^+$
$K^+\pi^+$
$K^-\pi^-$
b
$\pi^+\pi^+$
$K^-K^-$
$K^+K^+$
$\pi^-\pi^-$
c
$\pi^+\pi^-$
$K^+K^-$
$p\bar{p}$
d
$\bar{p}\pi^+$
$\bar{p}K^+$
$\bar{p}\pi^-$
$\bar{p}K^-$
e
$p\pi^-$
$pK^-$
$p\pi^+$
$pK^+$
f
$pp$
$\bar{p}\bar{p}$
σ.BR(mb)
Mass (GeV)
10
1
0.1
0.01
1.0
2.0
3.0
4.0
5.0

Fig. 6